JACUTINGAITE, Pt$_2$HgSe$_3$, A NEW PLATINUM-GROUP MINERAL SPECIES FROM THE CAUÊ IRON-ORE DEPOSIT, ITABIRA DISTRICT, MINAS GERAIS, BRAZIL

Anna VYMAZALOVÁ[§], František LAUFEK and Milan DRÁBEK

Czech Geological Survey, Geologická 6, CZ–152 00 Prague 5, Czech Republic

Alexandre Raphael CABRAL

Technical University of Clausthal, Mineral Deposits, Adolph-Roemer-Str. 2A, D–38678 Clausthal-Zellerfeld, Germany

Jakub HALODA and Tamara SIDORINOVÁ

Czech Geological Survey, Geologická 6, CZ–152 00 Prague 5, Czech Republic

Bernd LEHMANN

Technical University of Clausthal, Mineral Deposits, Adolph-Roemer-Str. 2A, D–38678 Clausthal-Zellerfeld, Germany

Henry Francisco GALBIATTI

*VALE S.A., Ferrous Planning and Development Department, Avenida de Ligação 3580,
34000-000 Nova Lima, Minas Gerais, Brazil*

Jan DRAHOKOUPIL

Institute of Physics of ASCR, Na Slovance 2, CZ–182 21 Prague 8, Czech Republic

Abstract

Jacutingaite, Pt$_2$HgSe$_3$, is a new species of platinum-group mineral discovered at the Cauê iron-ore deposit, Itabira district, Minas Gerais, Brazil. Observed in a polished section, the mineral is about 50 μm across and occurs on an aggregate of atheneite, potarite and hematite. The new mineral is partly altered to a Pt–O phase. Synthetic jacutingaite is megascopically grey in color, has a metallic luster and a grey streak. The mineral is brittle, with a very good {001} cleavage. Values of VHN$_{10}$ (15 indentations on five grains of synthetic Pt$_2$HgSe$_3$) are between 119 and 245 kg/mm^2, with a mean value of 169 kg/mm^2, corresponding to a Mohs hardness of approximately 3½. Under plane-polarized light, jacutingaite is light grey, has a moderate to distinct bireflectance, a bluish grey to rusty brown pleochroism, and a weak to distinct anisotropy; it does not exhibit internal reflections. Reflectance values of synthetic jacutingaite in air (R$_{max}$, R$_{min}$, in %) are: 51.1, 47.4 at 470 nm, 50.5, 48.2 at 546 nm, 49.6, 48.0 at 589 nm, and 47.8, 47.1 at 650 nm. Three electron-microprobe analyses of natural jacutingaite gave an average composition: Pt 37.30, Pd 5.91, Hg 25.72, Ag 0.16, Cu 0.82, and Se 31.48, total 101.39 wt.%, corresponding to the empirical formula (Pt$_{1.46}$Pd$_{0.42}$Cu$_{0.10}$Ag$_{0.01}$)$_{\Sigma1.99}$Hg$_{0.98}$Se$_{3.04}$ based on six atoms; the average result of nine analyses of synthetic jacutingaite is: Pt 47.14, Hg 24.24, and Se 28.62, for a total of 100.00 wt.%, corresponding to Pt$_{2.00}$Hg$_{1.00}$Se$_{3.00}$. The mineral is trigonal, space group $P\bar{3}m1$, with a 7.3477(2), c 5.2955(1) Å, V 247.59(1) Å^3 and Z = 2. The crystal structure was solved and refined from the powder X-ray-diffraction data on synthetic Pt$_2$HgSe$_3$. Jacutingaite is isostructural with Pt$_4$Tl$_2$X$_6$ (X = S, Se, or Te); no structural analogue is known as a mineral. Jacutingaite is structurally related to sudovikovite. The strongest lines in the X-ray powder-diffraction pattern of synthetic jacutingaite [d in Å(I)hkl] are: 5.2917(100)001, 2.7273(16)201, 2.4443(10)012, 2.0349(18)022, 1.7653(37)003, 1.3240(11)004 and 1.0449(11)025. The mineral is named after the specular-hematite-rich vein-type mineralization locally known as "jacutinga", in which it occurs.

Keywords: jacutingaite, platinum-group mineral, Pt–Hg selenide, electron-microprobe data, reflectance data, synthetic Pt$_2$HgSe$_3$, X-ray-diffraction data, crystal structure, Cauê deposit, Minas Gerais, Brazil.

[§] *E-mail address*: anna.vymazalova@geology.cz

Introduction

The new mineral species was first observed by Cabral *et al.* (2008) as the unnamed phase Pt_2HgSe_3 from the Cauê iron-ore deposit, Itabira district, Minas Gerais, Brazil. The mineral was discovered in a polished section of an aggregate, about 2 mm across, obtained from a heavy-mineral concentrate from a friable, hematite-rich vein. The mineral is named after the specular-hematite-rich vein-type gold mineralization locally known as "jacutinga". Jacutinga is characterized by palladiferous gold, together with Pd and Pt minerals in hematite–quartz–(talc–kaolinite) veins, which typically occur in some iron-ore deposits in the Quadrilátero Ferrífero of Minas Gerais, Brazil (*e.g.*, Henwood 1871, Hussak 1904, Cabral *et al.* 2009).

The mineral and the mineral name have been approved by the Commission on New Minerals, Nomenclature and Classification of the IMA (CNMNC 2010–078). The holotype specimen (polished section) is deposited in the collections of GeoMuseum "Geosammlung" at the Technical University of Clausthal, Adolph-Roemer-Str. 2A, D–38678 Clausthal-Zellerfeld, Germany, under catalogue number 26580. We here describe the properties of the new species, jacutingaite, and define its crystal structure.

Occurrence and Associated Minerals

The new mineral species, jacutingaite, was recovered from hematite-rich auriferous veins locally known as jacutinga in Minas Gerais. Such predominantly brittle veins cross-cut the ductile tectonic foliation of the host itabirite (metamorphosed Fe formation composed of alternating laminae of Fe oxides and quartz) at the Cauê iron-ore deposit, Itabira (*e.g.*, Galbiatti *et al.* 2007), the type locality of jacutingaite, and elsewhere in the Quadrilátero Ferrífero (Fig. 1; *e.g.*, Hussak 1904, Cabral *et al.* 2009). Another Hg-bearing Pt mineral is known from jacutinga in Itabira: hongshiite, ideally PtCu (*e.g.*, Cabral *et al.* 2008). The presence of barite inclusions in hongshiite and the use of Na–K – Na–Li fluid–mineral geothermometers indicate that oxidized brines of evaporitic origin interacted with the host itabirite at a maximum temperature of about 350°C (Lüders *et al.* 2005). This temperature constraint and the cross-cutting field relationships between jacutinga and the itabirite country-rock invalidate previous inferences that the jacutinga emplacement was synchronous with the peak of thermal metamorphism at 600°C and ductile deformation (Olivo *et al.* 1995).

Experimental Procedures

The single grain of jacutingaite hitherto observed and its small size prevented the extraction and isolation of the mineral in a sufficient amount for crystallographic and structural investigations, density measurement and

determination of physical properties. Therefore, these measurements were performed on synthetic Pt_2HgSe_3.

The synthetic Pt_2HgSe_3 phase was prepared using Kullerud's evacuated silica-glass-tube method (Kullerud 1971) in the Laboratory of Experimental Mineralogy of the Czech Geological Survey in Prague. Platinum (99.95%), mercury (99.999%) and selenium (99.999%), obtained from Johnson Matthey Co. Ltd., were the starting materials for synthesis. A carefully weighed sample was loaded into the high-purity silica tube, and a tightly fitting silica-glass rod was placed on top of the reagents in order to keep the charge in place and also to reduce the volume of vapor on heating. The evacuated tube with its charge was sealed and then annealed at 1200°C for three days. After cooling in a cold-water bath, the charge was meticulously removed from the tube, ground to powder in acetone using an agate mortar, and thoroughly mixed to homogenize it. The pulverized charge was sealed in an evacuated silica-glass tube again and reheated at 800°C for 840 hours and 400°C for 1704 hours. Temperature was controlled electronically (±4°C). The experimental product was rapidly quenched in a cold-water bath. According to the powder X-ray diffraction and electron-microprobe data, the experimental products at 800° and 400°C were identical.

Physical and Optical Properties

Jacutingaite occurs as a single grain about 50 μm across (Fig. 2) on an aggregate of atheneite, potarite and hematite. It is partly altered to a Pt–O phase (Cabral *et al.* 2008). Synthetic jacutingaite is grey in color, opaque, has a metallic luster and a grey streak. The mineral is brittle, with a very good {001} cleavage. Values of VHN_{10} (15 indentations on five grains of synthetic Pt_2HgSe_3) are between 119 and 245 kg/mm^2, with a mean value of 169 kg/mm^2, corresponding to a Mohs hardness of approximately 3½. The density calculated on the basis of the empirical formula is 10.35 g/cm^3. The density measured by weighing in toluene is 10.9 g/cm^3. Under plane-polarized light, jacutingaite and synthetic Pt_2HgSe_3 are light grey, have moderate to distinct bireflectance, bluish grey to rusty brown pleochroism, and a weak to distinct anisotropy; they exhibit no internal reflections.

Reflectance values of natural and synthetic jacutingaite were measured in air using an Ortholux Pol I (Leitz) microscope equipped with a photomultiplier MPV–1 (Leitz) and a Veril S–200 transmission-interference filter (Leitz), and a WTiC reference material. These were performed with ×44 objective and the numerical aperture was confined to 0.65. The reflectance data are given in Table 1. Figure 3 shows the reflectance curves of natural and synthetic jacutingaite. The slight difference in data for natural and synthetic jacutingaite may be caused by the palladium content of the natural sample.
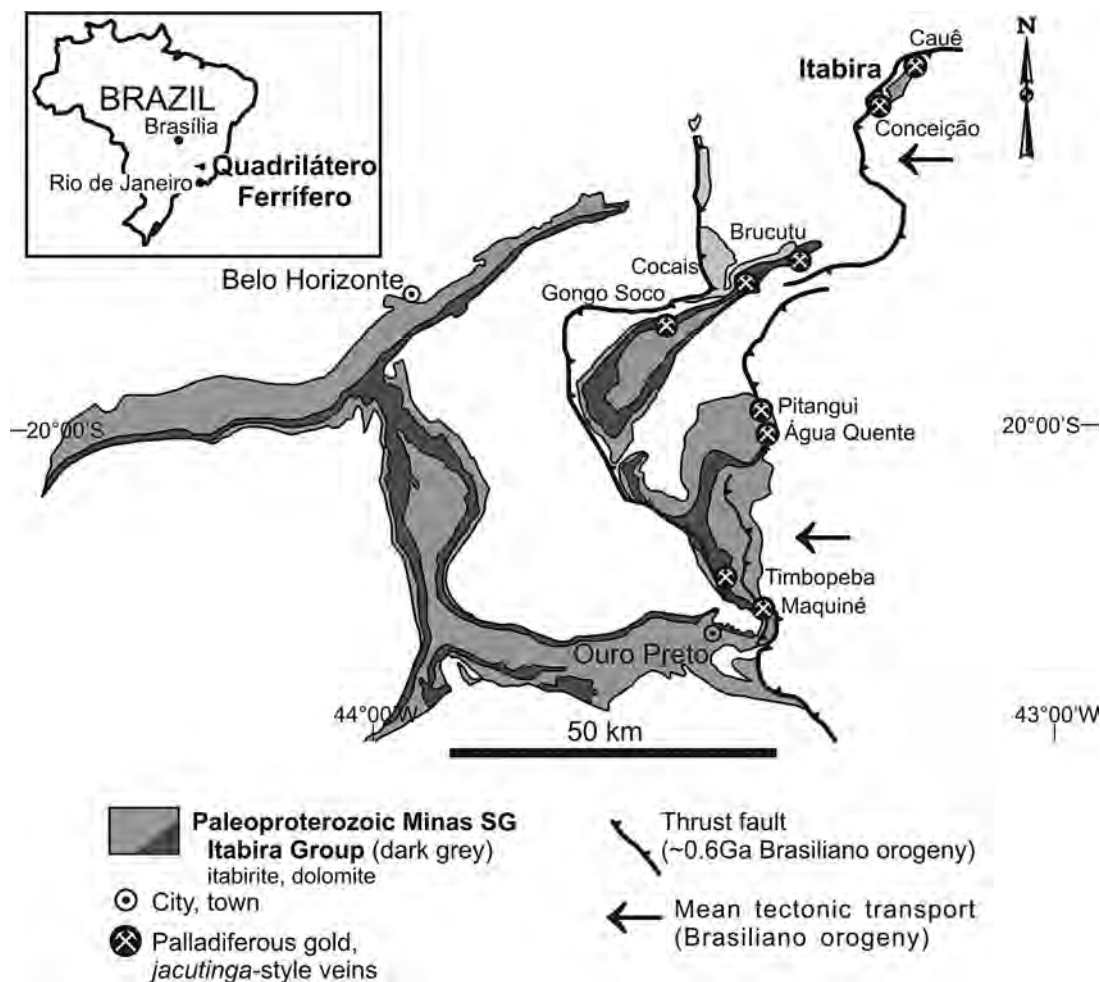
FIG. 1.   Geological overview of the Minas Supergroup of the Quadrilátero Ferrífero of Minas Gerais, Brazil, showing the location of the Cauê iron-ore deposit in the Itabira district and other localities where hematitic auriferous veins known as jacutinga occur [adapted from Cabral *et al*. (2009) and references therein]. The distribution of jacutinga occurrences delineates a north-trending, platiniferous Au–Pd belt that parallels the trace of major thrust faults. The belt continues northward following the trace of the thrust faults, which evolved during the ~0.6-Ga Brasiliano orogeny. This orogenic overprint produced the pervasive tectonic foliation observed in supracrustal rocks (*e.g*., Chemale *et al*. 1994). The hematite-rich Au–Pd–Pt-bearing jacutinga-style veins cross-cut the tectonic foliation of the host itabirite, indicating a late Brasiliano age.

CHEMICAL DATA

Chemical analyses of synthetic jacutingaite were performed with a Cameca SX–100 electron microprobe using the wavelength-dispersion mode. Acceleration voltage was set to 15 keV, and the beam current was 10 nA. The X-ray lines and reference materials were as follows: Pt$M\alpha$, Hg$M\alpha$ and Se$L\alpha$; pure metals (Pd, Se) and HgS. The electron-microprobe results are given in Table 2, together with those for natural jacutingaite (Cabral *et al*. 2008). The empirical formula (based on six

atoms) for natural jacutingaite (average result of three analyses) is $(Pt_{1.46}Pd_{0.42}Cu_{0.10}Ag_{0.01})_{\Sigma 1.99}Hg_{0.98}Se_{3.04}$, and for synthetic jacutingaite (average result of nine analyses), it ideally corresponds to $Pt_{2.00}Hg_{1.00}Se_{3.00}$.

CRYSTALLOGRAPHIC DATA

The availability of only one grain of the mineral and its small size prevented extraction and investigations by means of X-ray diffraction. Therefore, the relevant crystallographic and structural investigations

were performed on synthetic Pt₂HgSe₃. Observations by scanning electron microscopy showed that the crystals of synthetic Pt₂HgSe₃ form laminated particles suggestive of a layered structure, the typical grain-size of which is about 50 μm. Our attempts to prepare a single crystal suitable for single-crystal X-ray diffraction (*e.g.*, annealing in the presence of KI flux, vapor transport using iodine as a transport agent) were unsuccessful. Thus, the crystal structure of Pt₂HgSe₃ was determined from powder X-ray-diffraction data *ab initio*.

The X-ray-diffraction pattern used for structure determination was collected in the Bragg–Brentano geometry on an X´Pert Pro PANalytical diffractometer, equipped with X´Celerator detector and a Co*K*α radiation source. The data were collected in the range between 4 and 160° 2θ; a full width at half maximum of 0.090° in 2θ was obtained at 19.45° 2θ, indicating a good crystallinity of the sample. The details of data collection and basic crystallographic data are given in Table 3.
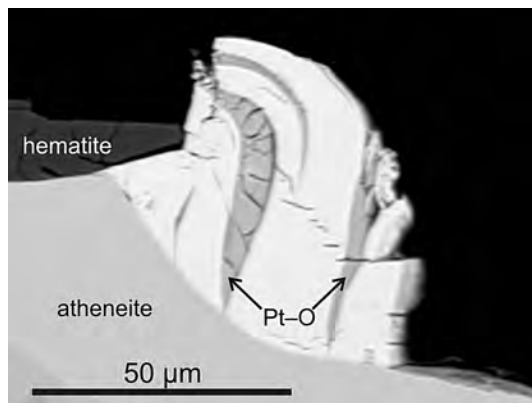

Fig. 2. Back-scattered electron image of jacutingaite (white) on the surface of an aggregate of hematite, potarite and atheneite.

TABLE 1. REFLECTANCE VALUES
FOR NATURAL AND SYNTHETIC JACUTINGAITE

λ (nm)	natural		synthetic	
	R_{max} (%)	R_{min} (%)	R_{max} (%)	R_{min} (%)
420	50.0	45.6	48.8	41.4
440	50.6	46.3	49.4	42.0
460	51.0	47.1	49.8	42.6
470	**47.4**	**51.1**	**42.9**	**50.0**
480	51.1	47.7	50.2	43.2
500	51.1	48.0	50.1	43.7
520	50.8	48.2	49.9	44.2
540	50.6	48.2	49.7	44.8
546	**48.2**	**50.5**	**44.9**	**49.8**
560	50.3	48.2	49.5	45.2
580	49.9	48.1	48.9	45.5
589	**48.0**	**49.6**	**45.6**	**48.6**
600	49.3	47.9	48.3	45.7
620	48.8	47.7	47.6	45.6
640	48.1	47.3	46.5	45.2
650	**47.1**	**47.8**	**45.0**	**46.0**
660	47.5	46.8	45.4	44.7
680	46.9	46.3	44.3	43.8
700	46.2	45.7	43.0	42.5

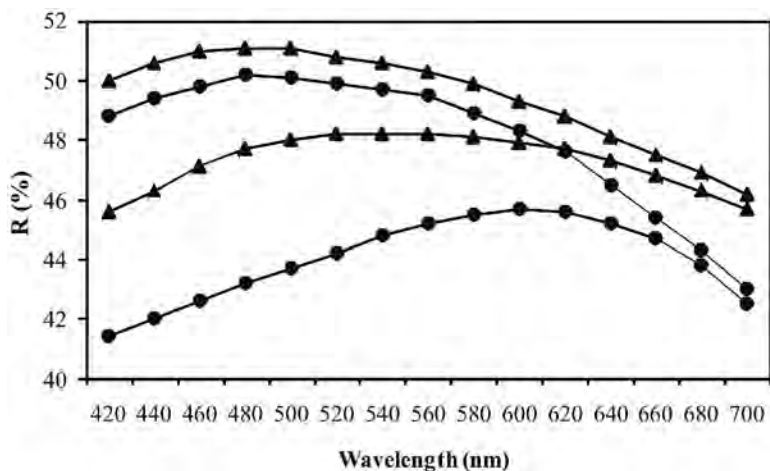The standard wavelengths (COM), shown in bold, were interpolated.

Fig. 3. Reflectance data for natural jacutingaite (triangles) compared to synthetic jacutingaite (circles) in air. The reflectance values (R %) are plotted *versus* λ wavelength in nm.

The indexing of the X-ray powder pattern was performed using the DICVOL04 program (Boultif & Louër 2004). The first 20 lines, with the exception of two weak diffraction peaks attributable to $PtSe_2$ (~2 wt.% from Rietveld analysis) as an impurity phase, were indexed on the basis of the trigonal cell with lattice parameters listed in Table 3. The figures of merit for assessing the quality of the solution are: $M_{20} = 198$ (de Wolff 1968) and $F_{20} = 123$ (0.0044;37) (Smith & Snyder 1976).

The crystal structure of Pt_2HgSe_3 was further refined by the Rietveld method for the powder X-ray-diffraction data by means of the program FULLPROF (Rodríguez-Carvajal 2006). The starting structural model for Pt_2HgSe_3 was derived from the published data for the synthetic phase $Pt_4Tl_2Se_6$ (Bronger & Bonsmann 1995), which has very similar lattice parameters (a 7.40, c 5.70 Å) and analogous stoichiometry. The initial structure model of Pt_2HgSe_3 ($Z = 2$) was obtained by replacement of Tl atoms by Hg atoms in the $Pt_4Tl_2Se_6$ ($Z = 1$) structure.

The pseudo-Voigt function was used to generate the shape of the diffraction peaks in the subsequent Rietveld refinement. The background was determined by the linear interpolation between consecutive breakpoints in the pattern. The refined parameters include those describing the peak shape and width, peak asymmetry, unit-cell parameters, fractional coordinates, preferred orientation along [001] and isotropic displacement parameters. Finally, 16 parameters were refined. The final cycles of refinement converged to the residual factors $R_{Bragg} = 0.076$, $R_{wp} = 0.044$ and $R_p = 0.029$. The crystal-structure data are given in Table 4, and the final

Rietveld plot and the crystal structure are presented in Figures 4, 5 and 6. The presentation of the stoichiometry of jacutingaite as Pt_2HgSe_3 with $Z = 2$ contrasts with its isostructural phases $Pt_4Tl_2S_6$, $Pt_4Tl_2Se_6$, $Pt_4Tl_2Te_6$ and $Pd_4Tl_2Se_6$, with $Z = 1$. Nevertheless, we have decided in favor of this type of presentation, as it is in accordance with the empirical chemical composition of this phase given by Cabral *et al.* (2008).

We present in Table 5 an indexed powder-diffraction pattern of jacutingaite.

DESCRIPTION OF THE STRUCTURE

Jacutingaite (Pt_2HgSe_3) is isostructural with the synthetic phases $Pt_4Tl_2S_6$, $Pt_4Tl_2Se_6$, $Pt_4Tl_2Te_6$ and $Pd_4Tl_2Se_6$, all described by Bronger & Bonsmann (1995). The unit cell of jacutingaite contains two Pt positions (four atoms), one Hg position (two atoms) and one Se position (six atoms). The Pt(1) atoms show an octahedral coordination with Se atoms, with Pt(1)–Se distances of 2.648(3) Å, whereas the Pt(2) atoms are surrounded by four Se atoms in a square planar coordination, with a Pt(2)–Se distance of 2.430(3) Å. In addition to the four Se atoms, each Pt(2) atom has two short contacts, with Hg atoms at a distance of 2.819(1) Å. Consequently, the complete coordination sphere of Pt(2) atoms can be described as an elongate octahedron $[Pt(2)Hg_2Se_4]$ having Hg atoms in a *trans* position with respect to one another. As indicated in Figure 5, the $[Pt(1)Se_6]$ octahedra share six Se–Se edges with adjacent $[Pt(2)Se_4]$ squares forming layers oriented parallel to (001). The Hg atoms are positioned in anti-cubo-octahedral voids (defined by Se atoms) between these

TABLE 2. ELECTRON-MICROPROBE DATA
FOR NATURAL AND SYNTHETIC JACUTINGAITE

	Mean	Range		Std. dev.	Standard
		Min	Max	σ	
a) **Natural material**: three analyses					
Pt wt.%	37.30	36.64	37.78	0.48	Pt metal
Pd	5.91	5.40	6.70	0.56	Pd metal
Hg	25.72	25.62	25.84	0.09	HgTe
Ag	0.16	0.20	0.29	0.09	Ag metal
Cu	0.82	0.52	0.97	0.21	$CuFeS_2$
Se	31.48	31.38	31.62	0.10	Se metal
Total	101.39				
b) **Synthetic material**: seven analyses					
Pt	46.73	45.86	47.53	0.53	Pt metal
Hg	24.06	23.44	25.31	0.53	HgS
Se	28.33	27.84	28.54	0.22	Se metal
Total	99.12				

The data on the natural sample are taken from Cabral *et al.* (2008).

TABLE 3. JACUTINGAITE: DATA COLLECTION
AND RIETVELD ANALYSIS

Data collection	
Radiation type, source	X-ray, Co$K\alpha$
Generator settings	40 kV, 30 mA
Range in 2θ (°)	4 – 160
Step size (°)	0.02
Crystal data	
Space group	$P\bar{3}m1$ (no. 164)
Unit-cell content	Pt_2HgSe_3, $Z = 2$
Unit-cell parameters (Å)	a 7.3477(2), c 5.2955(1)
Unit-cell volume (Å³)	247.59(1)
Rietveld analysis	
No. of reflections	148
No. of structural parameters	8
No of. profile parameters	5
R_F	0.073
R_{Bragg}	0.076
R_p	0.029
R_{wp}	0.044
Weighting scheme	$1/y_o$

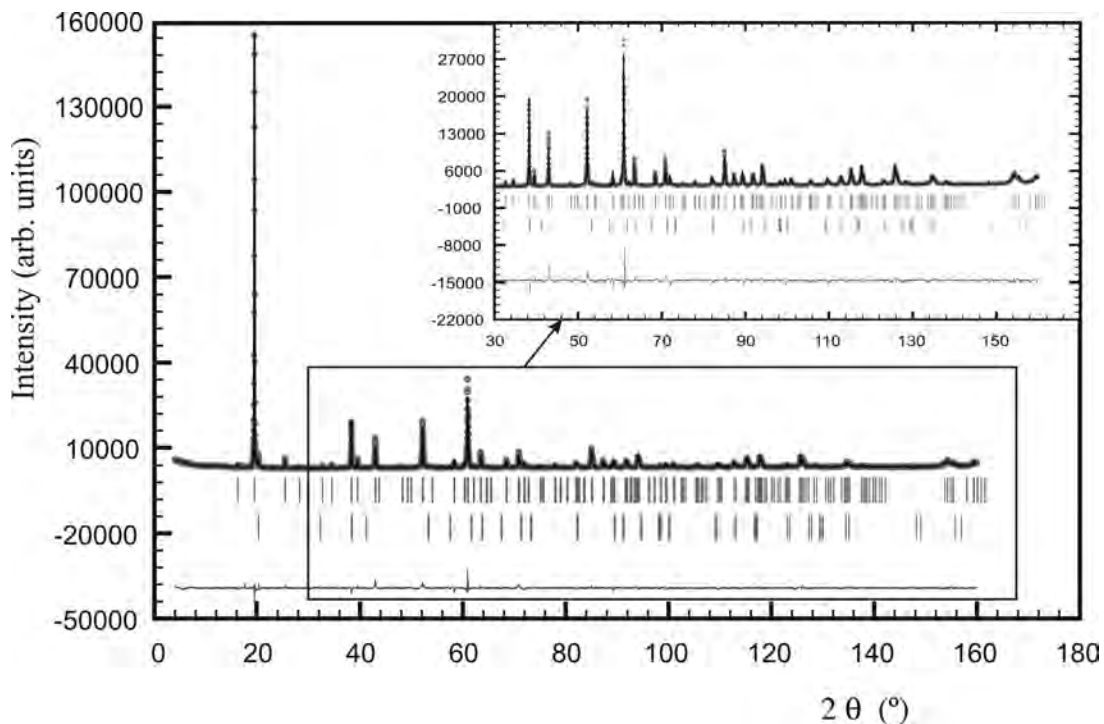The R agreement factors defined according to McCusker *et al.* (1999).

FIG. 4.   The observed (circles), calculated (solid line) and difference Rietveld profiles for jacutingaite. The upper reflection markers correspond to jacutingaite, and the lower markers, to 2 wt.% PtSe$_2$ impurity.
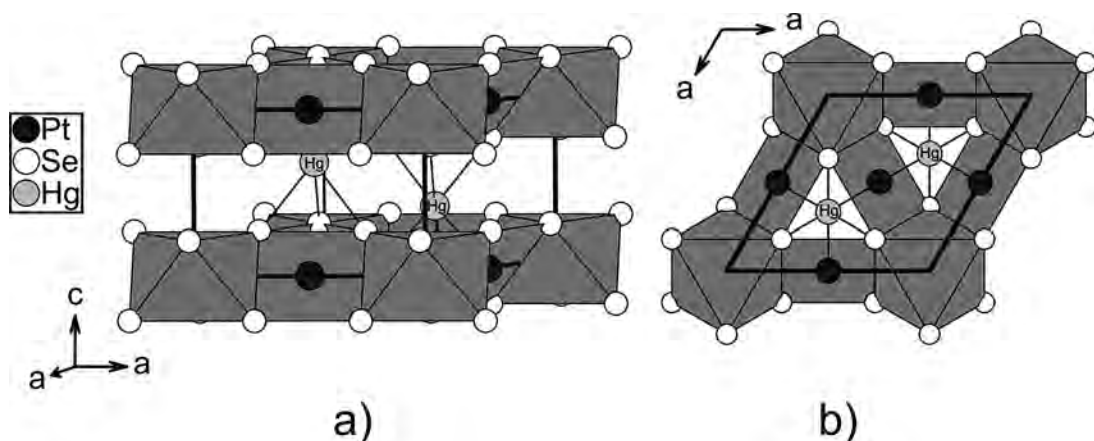

FIG. 5.   Polyhedral representation of the jacutingaite structure emphasizing the [Pt(1)Se$_6$] octahedra and [Pt(2)Se$_4$] squares. (a) Perspective view, (b) view along the **c** axis. The unit-cell edges are highlighted.

layers. More specifically, the Hg atoms are displaced along the **z** axis from the sheets of Pt atoms toward three Se atoms of the next structural layer. As a result, the closest coordination sphere of Hg atoms consists of three Pt(2) and three Se atoms showing an elongate octahedral arrangement. The layered character of the

crystal structure is in accordance with the observed cleavage of jacutingaite along {001} and the laminated morphology of crystals of synthetic Pt_2HgSe_3.

As mentioned by Bronger & Bonsmann (1995) for the isostructural compounds $Pt_4Tl_2X_6$ (X = S, Se, or Te), the Se atoms in the crystal structure of jacutingaite are arranged in layers perpendicular to the **c** axis, forming the *Kagomé* nets (Fig. 6). These nets show AB stacking sequence along the **c** axis. The layered structure of jacutingaite shows many similarities to that of sudovikovite (PtSe₂, $P\overline{3}m1$) (Furuseth *et al.* 1965), which crystallizes in the CdI_2-type structure and belongs to the melonite group within the Strunz mineralogical

system. Both minerals display the same symmetry, and their unit-cell volumes show the apparent relationship: $V(Pt_2HgSe_3) \approx 4V(PtSe_2)$. Moreover, the crystal structure of jacutingaite can easily be derived from that of sudovikovite (Fig. 7a) in two consecutive steps. In the first step, one quarter of the Se atoms in the $PtSe_2$ structure is replaced by Hg atoms (Fig. 7b). As a consequence, the stoichiometry of this hypothetical phase changes from Pt_4Se_8 to $Pt_4Hg_2Se_6$. In the second step, the Hg atoms are displaced from the sheets of Pt atoms (Fig. 7c) toward three Se atoms of the next structural layer (see above). It is also interesting to note that the space group of jacutingaite is a *k*-subgroup, listed as II*c* with *a* = 2*a'*, *c* = *c'* in the *International Tables for Crystallography, vol.* A (Hahn 1983), in the space group of sudovikovite.

TABLE 4. POSITIONS AND ISOTROPIC DISPLACEMENT PARAMETERS OF ATOMS IN SYNTHETIC JACUTINGAITE*

Atom	Wyckoff letter	x	y	z	B_{iso} (Å²)
Pt(1)	1a	0	0	0	0.44(2)
Pt(2)	3e	½	0	0	0.44(2)
Se(1)	6i	0.8196(5)	0.1804(5)	0.2492(2)	0.63(5)
Hg(1)	2d	⅓	⅓	0.3507(3)	0.29(5)

* Space group $P\overline{3}m1$.

PROOF OF IDENTITY OF NATURAL AND SYNTHETIC JACUTINGAITE

The structural identity between the synthetic Pt_2HgSe_3 and jacutingaite was confirmed by electron back-scattering diffraction (EBSD). For that purpose, we used a CamScan CS 3200 scanning electron microscope combined with a NORDLYS II EBSD system by HKL Technology, Denmark. The natural sample
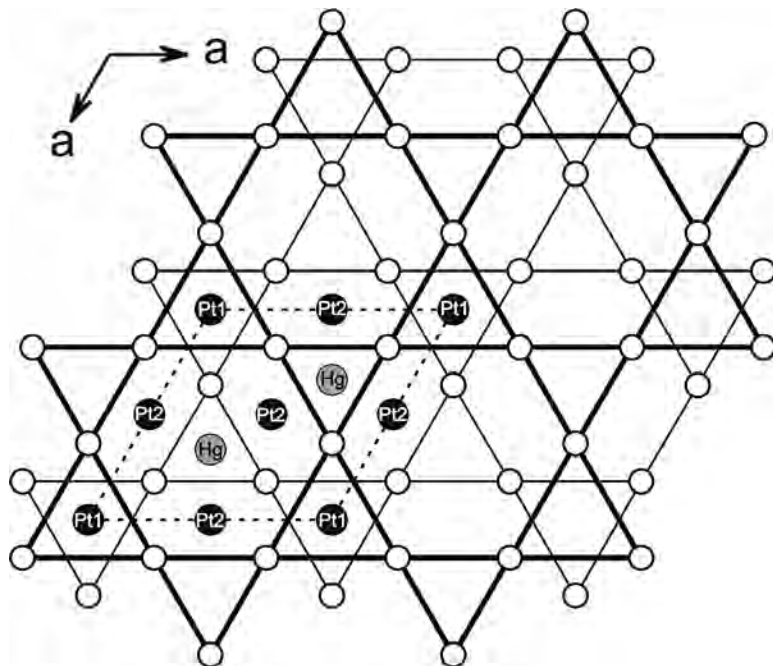

FIG. 6. View along the **c** axis showing two consecutive Kagomé nets of Se atoms (the thick and thin lines) in the crystal structure of jacutingaite. Note the AB-type stacking of Se atoms, and the octahedral and square planar coordinations of Pt(1) and Pt(2) atoms by Se, respectively. Unit-cell edges are indicated by dashed lines.

was prepared for investigation by etching the mechanically polished surface with colloidal silica suspension (OP–U) for 30 min. to reduce the surface damage. The EBSD patterns were collected and processed using a proprietary computer program CHANNEL 5 provided
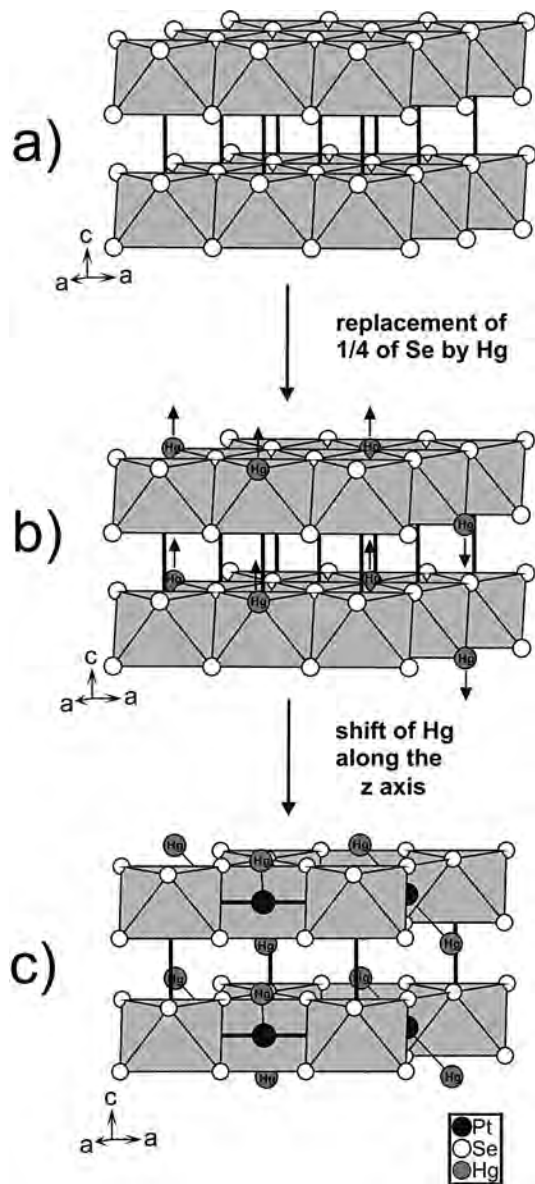

FIG. 7. Polyhedral representation showing relationship between the structure of jacutingaite (Pt_2HgSe_3) and sudovikovite ($PtSe_2$). The [$PtSe_6$] octahedra are highlighted. (a) Four unit cells of sudovikovite. (b) The hypothetical structure indicating the Se–Hg replacement and the shift of Hg atoms. (c) The jacutingaite structure.

TABLE 5. X-RAY POWDER-DIFFRACTION DATA
FOR SYNTHETIC JACUTINGAITE

I_{calc}	I_{obs}	d_{calc}	d_{obs}	h	k	l
100	**100**	5.2956	**5.2917**	0	0	1
2	2	4.0704	4.0684	0	1	1
<1		4.0704		1	0	1
17	**16**	**2.7273**	**2.7272**	**2**	**0**	**1**
<1		2.7273		0	2	1
2	2	2.6478	2.6471	0	0	2
3	**10**	2.4446	**2.4443**	0	1	2
5		2.4446		1	0	2
14	**18**	2.0352	**2.0349**	0	2	2
4		2.0352		2	0	2
4	6	1.8369	1.8367	2	2	0
1	1	1.7803	1.7803	1	2	2
<1		1.7803		2	1	2
36	**37**	1.7652	**1.7653**	0	0	3
6	7	1.701	1.7007	1	0	3
<1		1.701		0	1	3
3	3	1.5911	1.5909	1	1	3
<1		1.5908		4	0	0
5	7	1.5435	1.5435	0	2	3
1		1.5435		2	0	3
3	2	1.5236	1.5236	0	4	1
<1		1.5236		4	0	1
2	3	1.3636	1.3638	4	0	2
1		1.3636		0	4	2
11	**11**	**1.3239**	**1.3240**	**0**	**0**	**4**
3	4	1.2961	1.2962	0	1	4
5	5	1.2728	1.2728	2	2	3
4	5	1.2455	1.2455	1	1	4
2	9	1.2223	1.2223	0	2	4
6	6	1.0591	1.0591	0	0	5
1		1.0950		3	1	4
<1		1.0590		1	3	4
5	**11**	1.0447	**1.0448**	0	1	5
5		1.0447		1	0	5
5	**11**	1.0449	**1.0449**	0	2	5
4		1.0449		2	0	5

Co$K\alpha$ radiation.

by HKL Technology. The center of six Kikuchi bands was automatically detected using the Hough transform routine (Schmidt *et al.* 1991), with a resolution of 50 (internal Hough resolution parameter in the HKL software). The solid angles calculated from the patterns were compared with a synthetic Pt_2HgSe_3 match containing 80 reflectors to index the patterns. The EBSD patterns (also known as Kikuchi bands) obtained from the mineral (eleven measurements on different spots on jacutingaite) were found to match the patterns generated from the structure of synthetic Pt_2HgSe_3 provided by our crystal-structure solution (Fig. 8). The values of the mean angular deviation (MAD, *i.e.*, goodness of fit of the solution) between the calculated and measured Kikuchi bands are between 0.556° and 0.243°. These values reveal a very good match; as long as values of mean angular deviation are less than 1°, they are considered as indicators of an acceptable fit (HKL Technology 2004).

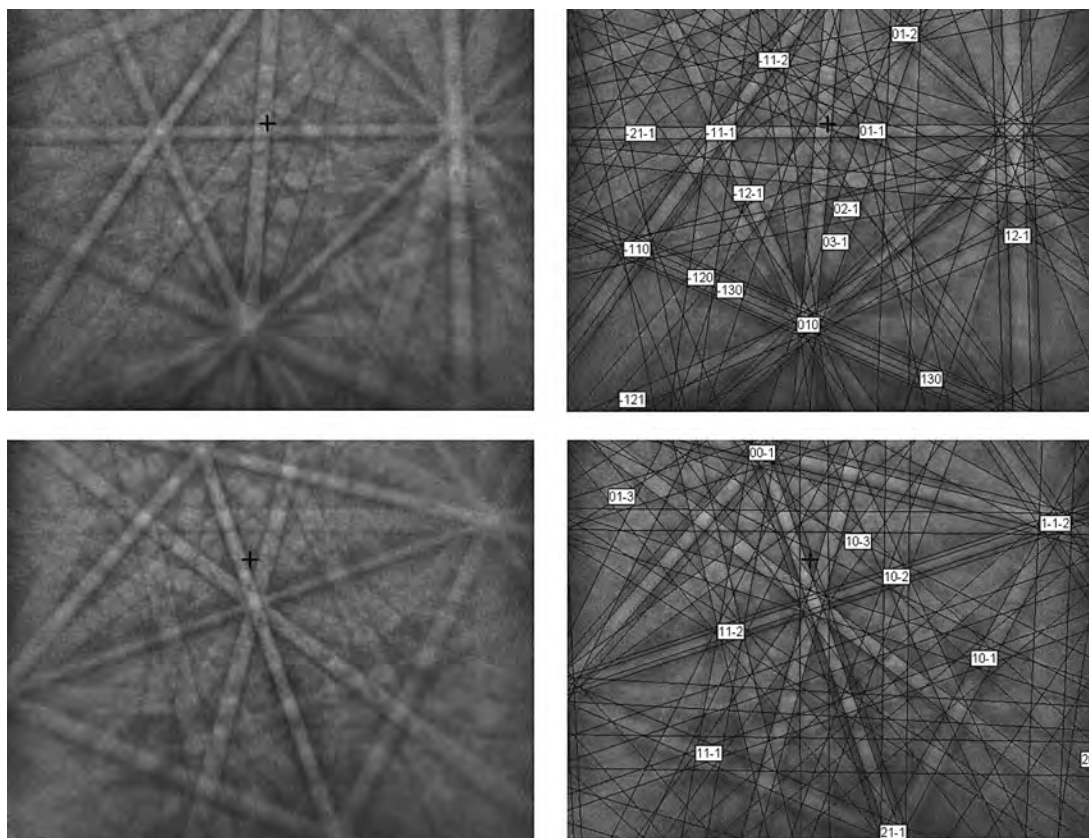The EBSD study, chemical identity and optical properties have confirmed that the natural and synthetic

Fig. 8.   EBSD images of natural jacutingaite; in the right column, the Kikuchi bands are indexed.

phases are the same. Consequently, our results render legitimate the use of the synthetic phase for the complete characterization of jacutingaite.

References

Boultif, A. & Louër, D. (2004): Powder pattern indexing with the dichotomy method. *J. Appl. Crystallogr.* **37**, 724-731.

Bronger, W. & Bonsmann, B. (1995): Ternäre Thallium-platin- und Thaliumpalladiumchalkogenide $Tl_2M_4S_6$. Synthesen, Kristallstruktur und Bindungsverhältnisse. *Z. Anorg. Allg. Chem.* **621** 2083-2088.

Cabral, A.R., Galbiatti, H.F., Kwitko-Ribeiro, R. & Lehmann, B. (2008): Platinum enrichment at low temperatures and related microstructures, with examples of hongshiite (PtCu) and empirical "Pt_2HgSe_3" from Itabira, Minas Gerais, Brazil. *Terra Nova* **20**, 32-37.

Cabral, A.R., Lehmann, B., Tupinambá, M., Schlosser, S., Kwitko-Ribeiro, R. & Abreu, F.R. de (2009): The platiniferous Au–Pd belt of Minas Gerais, Brazil, and genesis of its botryoidal Pt–Pd–Hg aggregates. *Econ. Geol.* **104**, 1265-1276.

Chemale, F., Jr., Rosière, C.A. & Endo, I. (1994): The tectonic evolution of the Quadrilátero Ferrífero, Minas Gerais, Brazil. *Precamb. Res.* **65**, 25-54.

de Wolff, P.M. (1968): A simplified criterion for reliability of a powder pattern indexing. *J. Appl. Crystallogr.* **1**, 108-113.

Furuseth, S., Selte, K. & Kjekshus, A. (1965): Redetermined crystal structures of NiTe$_2$, PdTe$_2$, PtS$_2$, PtSe$_2$. *Acta Chem. Scand.* **19**, 257-258.

Galbiatti, H.F., Fonseca, M.A., Pereira, M.C. & Polônia, J.C. (2007): Structural control of Au–Pd mineralization (Jacutinga): an example from the Cauê mine, Quadrilátero Ferrífero, Brazil. *Ore Geol. Rev.* **32**, 614-628.

Hahn, T., ed. (1983): *International Tables for Crystallography*, Volume A. Reidel Publishing Company, Dordrecht, The Netherlands.

Henwood, W.J. (1871): On the gold mines of Minas Geraes, in Brazil. *Trans. R. Geol. Soc. Cornwall* **8**, 168-370.

HKL Technology (2004): CHANNEL 5. HKL–Technology A/S, Hobro, Denmark.

Hussak, E. (1904): Über das Vorkommen von Palladium und Platin in Brasilien. *Sitz.-Ber. math.-naturwiss. Kl. Kais. Akad. Wiss.* **113**, 379-466.

Kullerud, G. (1971): Experimental techniques in dry sulfide research. *In* Research Techniques for High Pressure and High Temperature (G.C. Ulmer, ed.). Springer-Verlag, New York, N.Y. (288-315).

Lüders, V., Romer, R.L., Cabral, A.R., Schmidt, C., Banks, D.A. & Schneider, J. (2005): Genesis of itabirite-hosted Au–Pd–Pt-bearing hematite–(quartz) veins, Quadrilátero Ferrífero, Minas Gerais, Brazil: constraints from fluid inclusion infrared microthermometry, bulk crush-leach analysis and U–Pb systematics. *Mineral. Deposita* **40**, 289-306.

McCusker, L.B., von Dreele, R. B., Cox, D. E., Louër, D. & Scardi, P. (1999): Rietveld refinement guidelines. *J. Appl. Crystallogr.* **32**, 36-50.

Olivo, G.R., Gauthier, M., Bardoux, M., Sá, E.L., Fonseca, J.T.F. & Santana, F.C. (1995): Palladium-bearing gold deposit hosted by Proterozoic Lake Superior-type iron-formation at the Cauê iron mine, Itabira district, southern São Francisco craton, Brazil: geologic and structural controls. *Econ. Geol.* **90**, 118-134.

Rodríguez-Carvajal, J. (2006): FullProf.2k Rietveld Profile Matching & Integrated Intensities Refinement of X-ray and/or Neutron Data (powder and/or single-crystal). Laboratoire Léon Brillouin, Centre d´Etudes de Saclay, Gif-sur-Yvette Cedex, France.

Schmidt, N.H., Bildesorensen, J.B. & Jensen, D.J. (1991): Band positions used for online crystallographic orientation determination from electron back scattering patterns. *Scanning Microscopy* **5**, 637-643.

Smith, G.S. & Snyder, R.L. (1976): F_N: a criterion for rating powder diffraction patterns and evaluating the reliability of powder-pattern indexing. *J. Appl. Crystallogr.* **12**, 60-65.